

Doping mechanisms in stabilized amorphous Se films

K. TANAKA

Department of Applied Physics, Graduate School of Engineering, Hokkaido University, Sapporo, Japan

As- and Cl-doped, stabilized amorphous Se films have been utilized in photoconductive devices, while roles of the co-doping with a fixed As/Cl ratio remain speculative. We study the mechanism through analyses of structural and electronic energies in relevant Se clusters using *ab initio* calculations. The result suggests that, while sole doping of As and Cl causes gap states for holes and electrons, respectively, the co-doping produces -(As-Cl)- units in Se chains, which possess no gap states.

(Received September 20, 2016; accepted February 10, 2017)

Keywords: Selenium, Gap state, Photoconduction, Ab initio calculation, GAMESS

1. Introduction

Photoconductive applications of amorphous (a-) Se films have been growing from xerography [1,2] to sophisticated devices including avalanche vidicons and x-ray imagers [3,4]. These applications owe to the characteristic properties of a-Se, prominent photoconductivity and high dark-resistivity, the latter being inherent to the amorphous state. However, a disadvantage of pure a-Se is the thermal instability, i.e., crystallization upon long storage in humid atmospheres [1]. In order to suppress the instability, we commonly employ the so-called “stabilized a-Se film”, having dopants with typical concentrations of 0.2% As and 20-ppm Cl, which is deposited onto substrates held at temperatures T_s of $\sim 60^\circ\text{C}$ [5-7]. Such doping and preparation procedures seem to have been empirically selected [8], while despite of long usage of the films, the atomic structure and the doping mechanism remain elusive. It is also noted that Se can be regarded as the simplest lone-pair electron semiconductor [2,3], and understanding of doping mechanisms in the amorphous film is an invaluable subject in semiconductor science, which we will try to foster in the present work.

Stabilized a-Se films may be deposited as follows: It has been demonstrated that Se vapors consist mainly of Se_2 , Se_5 , and Se_6 clusters, the composition naturally varying with the temperature of an evaporating boat [1, 9-13]. Here, it remains vague whether these Se_n clusters with $n \geq 3$ take chain or ring forms in real situations, though calculations have asserted stability of rings [14-17]. In addition, how As and Cl dopants are contained in these Se clusters has neither been known. In any way, such clusters impinge upon metallic substrates held at T_s , $\sim 60^\circ\text{C}$ or annealed at $\sim 60^\circ\text{C}$ after deposition, wherein some structural relaxations will take place [18]. Since no electron-spin signals have been detected in dark-stored a-Se films [19] and glassy Se [20,21] as well (with estimated sensitivity of $\sim 10^{15}$ spin/cm $^{-3}$) and the films deposited at higher temperatures

are known to contain trigonal (t-) Se crystallites [1,22], it is plausible that the a-Se film with $T_s \approx 60^\circ\text{C}$ consists mainly of entangled chains [1-3,6,23,24]. Provided that the a-Se film resembles glassy Se, single chains may have $\sim 10^6$ atoms [1,3]. In more details, it has been demonstrated that film properties are affected by various factors, such as impurities [1,2,25], chemical forms of dopants [26], and preparation procedures of Se sources for evaporation [27], which add difficulties in preparation of the film with reproducible properties.

We here focus upon the doping effect of As and Cl into a-Se. It is straightforward to assume that a trivalent As ($4s^2p^3$) atom cross-links Se chains, which improves thermal stability through rising the crystallization [1] and glass-transition temperatures [28]. However, it is also known that the As doping tends to lengthen and shorten, respectively, electron and hole lifetimes [2,5,6,8,18], in which the reduction of the hole lifetime is fatal, since the holes, being more mobile than electrons in a-Se, govern the photoconduction. Then, to compensate the lifetime reduction, we may add Cl ($3s^2p^5$) with a ratio of 10^{-2} to As, while the co-doping mechanism remains vague [5-7]. Incidentally, sole doping of Cl atoms, which probably terminate Se chains [29], is demonstrated to reduce the electron range $\mu\tau$ (the drift mobility and the lifetime) with little effects upon the hole range [8, 30]. It should also be mentioned that, to the author's knowledge, no ESR studies concerning As and/or Cl doping have been reported, while the cross-linking and the terminating form are likely to generate no spin signals.

How can we understand these dopant effects on carrier transports? It is plausible that these behaviors are governed by gap states [7, 31], for which some ideas have been proposed. Conventional models assume some density modifications of dangling bonds by the dopants [2,5,6]. However, existence of the dangling bonds in a-Se has been questioned from several aspects [3]. In addition, the estimated density of native defects in a-Se is 10^{16} cm $^{-3}$ [32],

only $\sim 10^0$ ppm of the total atoms, which is much fewer than the dopant densities with the orders of 10^{-1} % As and 10^1 ppm Cl. It then seems valuable to examine alternative ideas. Hence, in the present study, we study the doping effects of As, Cl, and the co-doping with the specified ratio. Several Se clusters containing As and/or Cl are analyzed using an *ab initio* quantum chemical software, the result suggesting certain roles of As and Cl dopants and a co-doping mechanism. Specifically, the selected ratio $\sim 10^{-2}$ of Cl/As will be ascribed to suppression of chain-terminating As-Se ring structures.

2. Calculation

The present calculation employed a visualization platform Winmostar V5 [33] and an *ab initio* quantum chemical package GAMESS (1 May 2013 version) [34]. A selected base function was of the 6-31+G* type, and HF (Hartree-Fock) and B3LYP-DFT (Becke's three-parameter hybrid exchange functional and the Lee-Yang-Parr correlation function, Density Functional Theory)

approximations were adopted. These combinations have been demonstrated to provide quantitatively plausible results with acceptable computation times (≤ 1 day) [25]. Calculations were performed for several electronic parameters of small Se clusters, the structures being optimized through an energy-minimization procedure in GAMESS.

3. Results and discussion

3.1. Bond energy

At the outset, it may be in order to examine the bond energy under the present approximations. Table 1 compares the Pauling's bond energy [35] and the present results under the HF and DFT approximations. We see that the GAMESS-DFT results are more comparable to the empirically determined Pauling's values. In addition, the previous work has demonstrated that the DFT gives more plausible electronic properties [25]. Accordingly, we will adopt the DFT approximation hereafter.

Table 1. Bond energies [eV] of the listed atom combinations, given by Pauling and evaluated for the hydrates using GAMESS under HF and DFT approximations. For the GAMESS result of, e.g., Se-Se, the difference in the total energies between HSe-SeH and 2(HSe-) is tabulated

Bond, Unit	Pauling	GAMESS HF	GAMESS DFT
H-H	4.53	3.56	4.76
Se-Se, H-Se-Se-H	1.91	1.12	2.26
As-As, 2H=As-As=2H	1.40	1.14	2.07
Se-As, H-Se-As=2H	1.81	1.31	2.31
Se-Cl, H-Se-Cl	2.58	1.12	2.50
As-Cl, 2H=As-Cl	2.96	1.90	3.07

3.2. Pure Se

Before considering the doping effect, we need to model atomic and electronic structures of pure a-Se. Previous studies suggest that the atomic structure consists mostly of entangled, partially ring-like polymeric chains [1,2,23,24], for which the electronic structure may be estimated from analyses of elemental clusters. Accordingly, in Ref. 25, the author studied wavefunctions and energies of HOMO and LUMO levels, which correspond to the valence-band top and conduction-band bottom in solids, in several Se clusters, including helical H-*n*Se-H chains, Se_{*n*} rings, etc. Some results are replotted in Fig. 1.

We see that the structurally-optimized H-*n*Se-H gives consistent results with previous observation. Regarding the HOMO-LUMO gap, with increasing *n* it becomes narrower to ~ 3.5 eV, which is in harmony with the Tauc optical gap of ~ 2.0 eV in a-Se [1,2]. For the atomic structure, the Se-Se length *r*, bond angle θ and dihedral angle φ are, respectively, 2.37 Å, 107° and $\sim 80^\circ$, which are comparable with theoretical and experimental values in single chains, 2.4 ± 0.5 Å, $105 \pm 5^\circ$ and $80 \pm 5^\circ$ [36-41] and in t-Se, ~ 2.35 Å, $\sim 105^\circ$ and $\sim 102^\circ$ [24]; with a marked difference in the dihedral angles ($\sim 80^\circ$ and $\sim 103^\circ$) being attributable to interchain interaction. Concerning disorder effects, the analyses have demonstrated that the HOMO level is substantially influenced by fluctuations of the dihedral angle and the interchain separation, while the LUMO level varies with the length of chain segments.

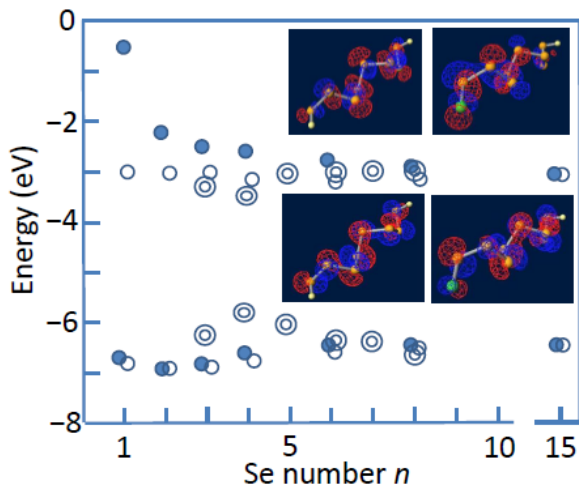


Fig. 1. HOMO (lower) and LUMO (upper) energies of helical $H-n\text{Se-H}$ (●), Se_n rings (⊙) and $H-n\text{Se-Cl}$ (○) chains as a function of n . The insets illustrate HOMO (lower) and LUMO (upper) wavefunctions of $H-8\text{Se-H}$ (left) and $H-8\text{Se-Cl}$ (right), in which the yellow, orange and green spheres depict H, Se and Cl, respectively

We also see in the figure that small Se_n rings with $n = 3 \sim 5$ produce smaller HOMO-LUMO gaps and the gaps in larger rings approach to that of the chains. The deviated HOMO and LUMO levels in the small rings arise, respectively, from stronger interaction between lone-pair states and from weaker σ^* (anti-bonding) interaction, which result from fairly planar ($\varphi \geq 125^\circ$) ring structures with long bond distances ($r \geq 2.39 \text{ \AA}$) and small bond angles ($\theta \leq 100^\circ$), the shape being consistent with the previous calculations [14-17]. Naturally, reflecting such strained structures, the total energy of the small rings is higher (more unstable) than that of the chain by $0.4 - 1.4 \text{ eV/ring}$, or $0.1 - 0.3 \text{ eV/atom}$. Hence, provided that Se films are thermally equilibrated at T_s ($\sim 60^\circ \text{C}$), the fraction of Se atoms forming such small rings (or ring-like curled chains) is estimated at $\sim 10^{-3}$. In larger rings (or ring-like chains), the short-range atomic structure is similar to that of the chain, with the dihedral angles of alternative signs [14-17], which gives rise to nearly the same HOMO-LUMO gaps, as shown in the figure. We also envisage that, in addition to the small rings (or ring-like chains), defective structures such as intimate valence-alternation pairs may exist [25]. It is hence plausible that, in pure a-Se, a few small ring(-like) and defective structures behave as carrier traps.

3.3. Cl effects

Fig. 1 also compares electronic levels and wavefunctions of the two kinds of chains, $H-n\text{Se-H}$ and $H-n\text{Se-Cl}$. We see different characters of the HOMO and LUMO levels.

The two HOMO levels are positioned at nearly the same energy, -6.5 eV , almost independent of n , with shallow hollows at $n \approx 2$. These resembling behaviors arise from the fact that the HOMO levels are governed by the lone-pair state of Se atoms, as shown in the insets. The interaction becomes minimal at $n \approx 2$, reflecting perpendicular lone-pair wavefunctions, which explains the hollows. The little Cl effect on the HOMO level in these clusters implies that the hole conduction in a-Se is mostly intact with the Cl doping, in consistent with unchanging hole $\mu\tau$ with Cl doping [8, 30].

On the other hand, the LUMO levels exhibit two contrastive behaviors. One is that the $H-n\text{Se-H}$ cluster manifests a dramatic energy decrease from $n = 1$ to ~ 4 , which approaches to a saturated value of -3.1 eV . This decrease is ascribable to extension of one-dimensional quantum wells produced by the σ^* wavefunctions lying along Se chains. By contrast, the $H-n\text{Se-Cl}$ cluster takes a lower, nearly-fixed LUMO level, at about -3.2 eV , which is dominated by the σ^* state of the terminal Se-Cl bond, as shown in the inset. Actually, additional calculations have demonstrated that the level is sensitive to the Se-Cl distance. Finally, it should be mentioned that the Mulliken's atomic charges of the $-\text{Se-H}$ and $-\text{Se-Cl}$ pairs in these chains are $-0.08/+0.11$ and $+0.09/-0.12$, with other Se being mostly neutral (≤ 0.01).

In short, the sole Cl doping into Se seems to exert two effects. One is that the lower LUMO level and the ionizing Cl clusters make the terminal $-\text{Se-Cl}$ an electron trap. The other is a topological effect that the Cl doping into a-Se probably assists to shorten Se chains, which may contribute more markedly to scission of the σ^* wavefunctions. These two factors appear to reduce $\mu\tau$ of electrons with hardly affecting hole transport, as experimentally demonstrated [5, 8, 30].

3.4. As effects

An As atom can be a nucleus generating several kinds of connections in a-Se, including triangular apexes extending three Se chains, $=\text{As-As}=\text{As}$ homopolar bonds, and so forth. Among those, what are interested in are relatively-stable structures which affect carrier transport through electronic and conformational effects. We will examine related clusters, taking $H-n\text{Se-H}$ as references.

It is reasonable to assume that high bond strength of As-Se (Table 1) makes As triangular pyramids the most abundant As-related structures. We model such connections by the pyramidal clusters, $\text{As}\equiv 3((n/3)\text{Se-H})$. Its stability has been examined through calculating the total energy, which demonstrates that $\text{As}\equiv 3((n/3)\text{Se-H})$ is more negative, i.e. stable, by $\sim 0.5 \text{ eV/unit}$ than that of an isolated system consisting of the same atoms, $\text{As}\equiv 3\text{H}$, $H-n\text{Se-H}$ and $-\text{H}_2$. The result implies that the As pyramid exists ubiquitously in As-doped a-Se, which may suppress the occurrence of unstable small ring(-like) structures.

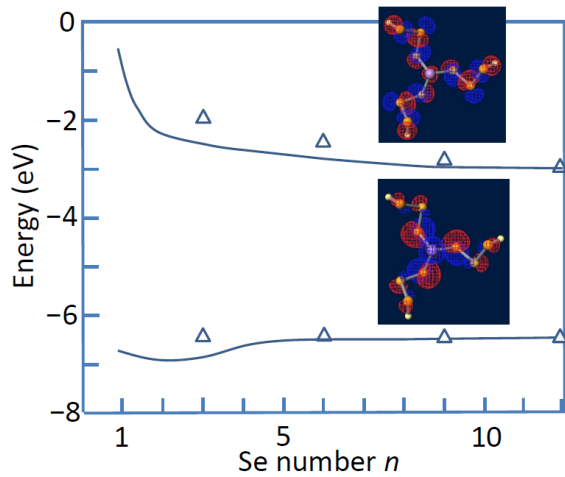


Fig. 2. HOMO and LUMO energies of $\text{As}\equiv 3(n/3)\text{Se-H}$ pyramid (Δ) in comparison with those of H-nSe-H (solid lines) as a function of the contained Se numbers n . The insets show HOMO and LUMO wavefunctions of a structurally-optimized $\text{As}\equiv 3(3\text{Se-H})$

On the other hand, as shown in Fig. 2, the pyramidal structures have the HOMO and LUMO levels at around -6.5 eV and -2.5 eV, the latter decreasing to -3.0 eV with n . The LUMO level is located at higher energies than the chain level, which seems to reflect a higher energy of the $\sigma^*(\text{As-Se})$ state than that of the $\sigma^*(\text{Se-Se})$. Concomitantly, the As-crosslinking enhances σ^* -bond networking, which may contribute to lengthen the electron lifetime, as experimentally demonstrated [6,8,18]. In contrast, the HOMO level is located at nearly the same energy with that of the chain, and accordingly, the As pyramid is assumed to cause little ill-effects on hole transport.

We then inspect other As-related structures. Fig. 3 summarizes the electronic energies and the structural instability ΔE , which is measured as the difference in the total energy from that of the As pyramid. Hence, in this representation, the pyramid is plotted by the two sun symbols at $\Delta E = 0$ with the HOMO and LUMO levels at -6.5 and -2.5 eV (Fig. 2). The two horizontal lines depict the two electronic levels of a reference chain with $n \approx 15$ (Fig. 1).

The As-As homopolar bond may be the first candidate. Total energy calculations have demonstrated, as shown by the double circles in Fig. 3, that the bond is located at $\Delta E \approx 0.23$ eV. Here, again assuming thermal equilibrium at 60°C ($k_B T \approx 30$ meV), we obtain $\exp(-\Delta E/k_B T) \approx 0.0005$ ($=0.05\%$), i.e., a very few, doped As atoms may form the homopolar bond. Incidentally, a typical purity of Se ingots employed in conventional experiments is, at most, 6-nine (10^{-6} impurity) [1, 21, 26], so that if the concentration of doped As is 0.2%, we can neglect the As-related structures fewer than 0.05% ($= 500\text{ppm}$), as indicated by the yellow arrow in Fig. 3. On the other hand, the HOMO level of the bond is located at nearly the same energy with that of the chain, the both being governed by the Se lone-pair states. By contrast, the LUMO level is located at higher positions, reflecting higher $\sigma^*(\text{As-As})$ states. In short, in a-Se, the

As-As homopolar bond may produce a barrier to electron motion while it hardly affects hole transport. Calculations have also demonstrated that As-related structures such as $-\text{As}=2\text{Se}=\text{As}-$ can be neglected due to scarcity.

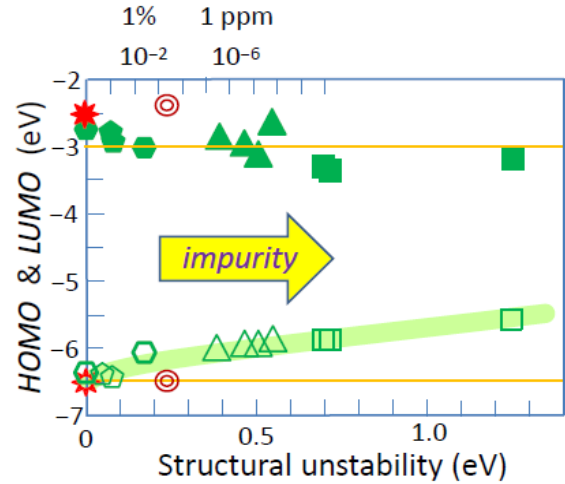


Fig. 3. Energy levels and structural instability ΔE , measured with reference to that of the As pyramid, of several As-Se clusters; As pyramid (sun), $=\text{As-As}=\text{}$ (double circle), $-\text{As}=2\text{Se}$ (triangle), $-\text{As}=3\text{Se}$ (square), $-\text{As}=4\text{Se}$ (pentagon), and $-\text{As}=5\text{Se}$ (hexagon). The two horizontal lines depict the HOMO and LUMO levels of the Se chain, and the upper scale represents a fractional existence ratio of the clusters, which is calculated under an assumption of thermal equilibrium at 60°C

Among a variety of As-related structures, As-mediated terminal rings $-\text{As}=m\text{Se}$ (Fig. 4) seem to play a key role. The electronic levels and ΔE naturally vary with m and are also modified by conformational variations of attaching Se chains, as represented by distributed same symbols. Nevertheless, as shown in Fig. 3, reflecting structural strains, ΔE tends to increase in smaller m clusters, with an inversion at $m = 2$ and 3, which is ascribable to unique conformations ($\theta \approx 60^\circ$ and 90°). On the other hand, the HOMO level tends to shift higher in smaller m clusters, which is due to enhanced lone-pair interaction resulting from paralleled wavefunctions, as illustrated in Fig. 4. By contrast, the LUMO level is roughly the same with that of the chain.

We here point out the importance of $-\text{As}=5\text{Se}$ terminal rings. As shown by the hexagons in Fig. 3, the fractional density of such rings is estimated at $\sim 1\%$ of the doped As, i.e., 10^{-5} of the total atom if the doped As density is 0.2%. And, the HOMO level is higher by ~ 0.5 eV than that of the chain. Needlessly, the level could be broadened in a-Se, due to disorder structures, while the effects on Se chains and the terminal rings are assumed to be of similar degrees. Accordingly, in a-Se, the terminal ring possibly works as a hole trap and shorten the hole lifetime, which is consistent with experimental observations [6, 8, 18].

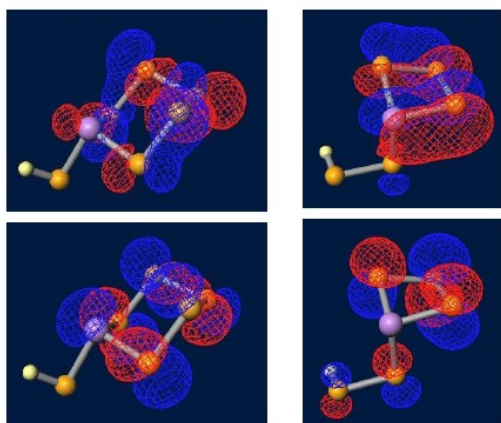


Fig. 4. HOMO (lower) and LUMO (upper) wavefunctions in $H\text{-Se-As}=5\text{Se}$ (left) and $H\text{-}2\text{Se-As}=3\text{Se}$ (right)

Finally, it would be valuable to note an As effect on O-contaminated Se. It is known [1] that the electrical resistivity of Se is surprisingly sensitive to ppm-order O-impurities, which may produce deep LUMO levels working as acceptors, while those can be compensated by As doping [25]. Such a compensation effect may contribute to lengthen the electron lifetime, as experimentally demonstrated [6,8,18].

3.5. Co-doping effects

When As and Cl are co-doped, since the As-Cl bond has the highest bond strength (Table 1), this bond suppresses preferentially the occurrence of more unstable As-related structures. And, if the density of Cl is $1/10^2$ of the As density, all the unstable As-structures with $\Delta E \geq 0.15$ eV, including $\text{-As}=m\text{Se}$ rings with $m \approx 5$ and =As-As= homopolar bonds, cannot appear (see, Fig. 3). In

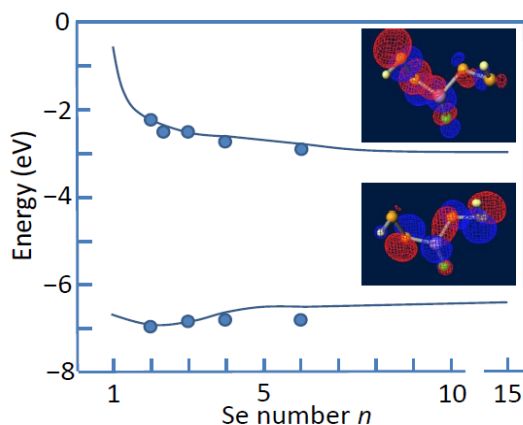


Fig. 5. HOMO and LUMO energies of $H\text{-}m\text{Se-(As-Cl)-}l\text{Se-H}$ with those in the helical $H\text{-}n\text{Se-H}$ chain as a function of the total Se number $n (= m + l)$, with the insets illustrating the HOMO and LUMO wavefunctions of an energy-optimized $H\text{-}2\text{Se-(As-Cl)-}2\text{Se-H}$ cluster

the ideal situation, there might exist only the As pyramids, which are harmless to hole transport, and As-Cl units.

Then, the last problem is “Where are the electronic levels of the As-Cl unit?” Fig. 5 shows that the HOMO and LUMO levels of $H\text{-Se...-(As-Cl)...Se-H}$ are located at around -6.8 eV and -2.5 eV, being lower than and similar to those of $H\text{-}n\text{Se-H}$ chains, respectively. Such situations arise from the facts that, as shown in the insets, the As-Cl unit tends to split and weaken the lone-pair interaction, while its effect upon the σ^* state seems secondary. As the result, the structure produces no hole traps, the result being in consistency with the observations [6].

4. Conclusions

We have studied the doping mechanism in stabilized Se films through *ab initio* calculations of electronic and structural energies in several Se clusters. As atoms with a concentration of $\sim 0.2\%$, which are incorporated into a-Se for improving thermal stability, nucleate various atomic structures, including As pyramids, which are the most common, =As-As= homopolar bonds, and $\text{-As}=m\text{Se}$ terminal rings. The last one, specifically $m \approx 5$ with a typical concentration of $\sim 1\%$ of the total doped As atoms, seems to cause fatal gap states for holes. Addition of 20-ppm Cl suppresses the occurrence of the terminal rings through producing As-Cl units, which can smear out the gap states.

The present cluster calculation has also revealed a general rule: the structural units having stronger lone-pair and weaker σ^* interactions, respectively, produce higher HOMO and lower LUMO states, which are likely to behave as hole and electron traps in disordered lone-pair semiconductors.

References

- [1] R. A. Zingaro, W. C. Cooper (eds.), Selenium (Van Nostrand Reinhold Company, New York, 1974).
- [2] N. F. Mott, E. A. Davis, Electronic Processes in Non-crystalline Materials 2nd ed., (Clarendon Press, Oxford, 1979).
- [3] K. Tanaka, K. Shimakawa, Amorphous Chalcogenide Semiconductors and Related Materials, (Springer, New York, 2011).
- [4] S. Kasap, J.B. Frey, G. Belev, O. Tousignant, H. Mani, J. Greenspan, L. Laperriere, O. Bubon, A. Reznik, G. DeCrescenzo, K. S. Karim, J. A. Rowlands, Sensors **11**, 5112 (2011).
- [5] D. M. Pai, J. Imaging Sci. Technol. **41**, 135 (1997).
- [6] S. O. Kasap, K. V. Koughia, B. Fogal, G. Belev, R. E. Johanson, Semiconductors **37**, 789 (2003).
- [7] S. Kasap, C. Koughia, J. Berashevich, R. Johanson, A. Reznik, J. Mater. Sci.: Mater. Electron. **26**, 4644 (2015).

- [8] J. Schottmiller, M. Tabak, G. Lucovsky, A. Ward, *J. Non-Cryst. Solids* **4**, 80 (1970).
- [9] J. P. Audiere, C. Mazieres, J. C. Carballes, *J. Non-Cryst. Solids* **27**, 411 (1978).
- [10] A. Motohashi, A. Kinoshita, *J. Non-Cryst. Solids* **95&96**, 1017 (1987).
- [11] K. Nagata, T. Hayakawa, M. Yao, H. Endo, *J. Non-Cryst. Solids* **205-207**, 807 (1996).
- [12] C. Bréchnignac, Ph. Cahuzac, N. Kébaïli, J. Leygnier, *J. Chem. Phys.* **112**, 10197 (2000).
- [13] K. Kooser, D.T. Ha, E. Itälä, J. Laksman, S. Urpelainen, E. Kukku, *J. Chem. Phys.* **137**, 044304 (2012).
- [14] D. Hohl, R. O. Jones, R. Car, M. Parrinello, *Chem. Phys. Lett.* **139**, 540 (1987).
- [15] Z. Q. Li, J. Z. Yu, K. Ohno, B. L. Gu, R. Czajka, A. Kasuya, Y. Nishina, Y. Kawazoe, *Phys. Rev. B* **52**, 1524 (1995).
- [16] A. Alparone, *Theor. Chem. Acc.* **131**, 1239 (2012).
- [17] W. Xu, W. Bai, *J. Mol. Struct. Theochem.* **854**, 89 (2008).
- [18] C. Allen, G. Belev, R. Johanson, S. Kasap, *J. Vac. Sci. Technol. A* **28**, 1145 (2010).
- [19] A. V. Kolobov, M. Kondo, H. Oyanagi, A. Matsuda, K. Tanaka, *Phys. Rev. B* **58**, 12004 (1998).
- [20] B. G. Bagley, F. J. DiSaovo, J. V. Waszczak, *Solid State Commun.* **11**, 89 (1972).
- [21] S. C. Agarwal, *Phys. Rev. B* **7**, 685 (1973).
- [22] E. Montrimas, B. Petrétis, *J. Non-Cryst. Solids* **15**, 96 (1974).
- [23] G. Lucovsky, in: *The Physics of Selenium and Tellurium*, E. Gerlach, P. Grosse (eds.), (Springer-Verlag, Berlin, 1979).
- [24] P. Andonov, *J. Non-Cryst. Solids* **47**, 297 (1982).
- [25] K. Tanaka, *J. Optoelectron. Adv. M.* **17**(11-12), 1716 (2015).
- [26] Y. Takasaki, E. Maruyama, T. Uda, T. Hirai, *J. Non-Cryst. Solids* **59&60**, 949 (1983).
- [27] K. Suzuki, K. Matsumoto, H. Hayata, N. Nakamira, N. Minari, *J. Non-Cryst. Solids* **95&96**, 555 (1987).
- [28] M. B. Myers, E.J. Felty, *Mat. Res. Bull.* **2**, 535 (1967).
- [29] D. Tonchev, S. O. Kasap, *Phys. Chem. Glasses* **43**, 66 (2002).
- [30] G. Belev, D. Tonchev, B. Fogal, C. Allen, S. O. Kasap, *J. Phys. Chem. Solids* **68**, 972 (2007).
- [31] F. Serdouk, M. L. Benkheldir, *Physica B* **459**, 122 (2015).
- [32] S. G. Bishop, U. Strom, P. C. Taylor, *Phys. Rev. B* **15**, 2278 (1977).
- [33] <http://winmostar.com/jp/>
- [34] M. W. Schmidt, K. K. Baldrige, J. A. Boatz, S. T. Elbert, M. S. Gordon, J. H. Jensen, S. Koseki, N. Matsunaga, K. A. Nguyen, S. J. Su, T. L. Windus, M. Dupuis, J. A. Montgomery, *J. Comput. Chem.* **14**, 1347 (1993).
- [35] L. Pauling, *The Nature of the Chemical Bond* 3rd ed., (Cornell Univ. Press, Ithaca, 1960).
- [36] M. Springborg, R. O. Jones, *J. Chem Phys.* **88**, 2652 (1988).
- [37] Y. Katayama, M. Yao, Y. Ajiro, M. Inui, H. Endo, *J. Phys. Soc. Jpn.* **58**, 1811 (1989).
- [38] A. Ikawa, H. Fukutome, *J. Non-Cryst. Solids* **117/118**, 328 (1990).
- [39] K. Hoshino, F. Shimojo, T. Nishida, *J. Phys. Soc. Jpn.* **68**, 1907 (1999).
- [40] P. Simoncic, T. Armbruster, *Microporous Mesoporous Mater.* **71**, 185 (2004).
- [41] A. Saitoh, K. Tanaka, *J. Appl. Phys.* **105**, 113530 (2009).

Corresponding author: keiji@eng.hokudai.ac.jp